ELSEVIER

Physica B 304 (2001) 339–347

PHYSICA B

www.elsevier.com/locate/physb

Some nonlinear properties of ferroelectric smart materials

Simon Dorfman[a], David Fuks[b], Alex Gordon[c,*], Eugene Kotomin[d], Peter Wyder[e]

[a] *Department of Physics, Technion – Israel Institute of Technology, 32000 Haifa, Israel*
[b] *Materials Engineering Department, Ben-Gurion University of the Negev, P.O. Box 653, 84105 Beer Sheva, Israel*
[c] *Department of Mathematics and Physics, Haifa University at Oranim, 36006 Tivon, Israel*
[d] *Institute of Solid State Physics, University of Latvia, Kengaraga Str. 8, Riga, LV-1063, Latvia*
[e] *Grenoble High Magnetic Field Laboratory, MPI-FKF, B.P. 166X-F-38042, Grenoble Cedex 9, France*

Received 5 February 2001

Abstract

Four types of nonlinear properties of ferroelectric smart materials have been considered: nonlinear dynamics of the paraelectric–ferroelectric interphase boundaries, nonlinear equilibrium excitations—domain walls, nonlinear response of the domain structure near the first-order phase transition—wetting of domain walls—and nonlinear effects caused by external high magnetic fields. The above mentioned nonlinearities have been studied in $(Ba,Sr)TiO_3$(BST) and $Pb(Zr,Ti)O_3$(PZT). © 2001 Elsevier Science B.V. All rights reserved.

Keywords: Ferroelectrics; Perovskites; Wetting; Kinetics; Phase transitions; Solid solutions

1. Introduction

Smart materials, including ABO_3 ferroelectric solid solutions, are multifunctional materials exploited in different fields of science and engineering. They feature a combination of sensors, actuators and processors. Some perovskites with ABO_3 have recently attracted attention as smart materials, i.e. as "very firm" ceramics, as substances having very large electrooptic coefficients and as materials applied in the development of integrated micromechanical transistor, memory, and optical devices [1–5]. The mechanical, electrical and optical properties of perovskite solid solutions depend strongly on the concentrations of their components. For this reason, it is important to investigate their properties which are sensitive to small changes of composition. The sensitivity of the perovskite-based devices depends crucially on the kinetics of the phase transitions in these substances. As a result of the concentration change of a component of the solid solution, the first-order phase transition is transformed into a second-order one at a tricritical point [6–10]. At a definite concentration, hydrostatic pressure and temperature range, the interphase boundary separating paraelectric and ferroelectric phases exists. Most of the work on ferroelectric perovskite solid solutions has focused on the research of their static properties while we emphasize here efficiency of investigations of phase transition kinetics due to its large sensitivity to composition changes of the solid solution. The aim of this paper is also to consider the effect of the wetting of domain walls in some perovskites. This effect was previously

*Corresponding author. Fax: +972-4-9832167.
E-mail address: algor@techunix.technion.ac.il (A. Gordon).

0921-4526/01/$ - see front matter
PII: S0921-4526(01)00504-X

discussed both for liquid–liquid and solid–liquid interfaces [11,12] near the phase transition temperature and expresses itself in the formation of the third phase, which is formed as a layer at the interface and is thermodynamically unstable in the bulk under the same conditions. In Ref. [13], the analytical form of the polarization profile of a domain wall near a first-order phase transition point was obtained and the influence of elastic forces on this phenomenon was studied. The effect of formation of a paraelectric layer of a finite thickness at the interface boundary which separates two ferroelectric domains with antiparallel direction of polarization vectors appears to be sensitive to the concentration of the element alloying the perovskite. We discuss this effect for $(Ba, Sr)TiO_3$(BST) and $Pb(Zr, Ti)O_3$(PZT) solid solutions. We show also for BST how the external magnetic field influences the wetting of domain walls. We conside concentration and magnetic field effects on the kinetics of phase transformations in perovskites in which phase transitions occur without diffusion. The influence of high magnetic fields on metastable states in ferroelectric phase transitions and on growth rates of paraelectric and ferroelectric phases is studied. The magnetic field influence on ferroelectric perovskites was observed in $BaTiO_3$ and $KTaO_3$ and was due to the magnetoelectric effect [14–16]. The growth and kinetics processes at symmetry-breaking first-order phase transitions are associated with the migration of interphase boundaries separating two coexisting phases. The objects of our research are ferroelectric perovskites in which magnetic field affects the mechanical, dielectric, piezoelectric, electrooptic and superconducting properties. Our calculations are based on the experimental data for BST and PZT solid solutions. We show that the velocity of the interphase boundary is very sensitive to concentration changes near the phase transition. The mean-field approximation used in our approach describes well many static and dynamic phenomena in ferroelectrics, for example, in perovskites discussed here [3]. For this reason, the theoretical results on the temperature-induced kinetics of perovskite ferroelectrics has been successfully used for the interpretation of experiments on the interphase boundary motion under isobaric conditions [17,18]. The application of the alloying-induced kinetics of ferroelectric phase transitions can be also useful for the interpretation of corresponding hydrostatic pressure measurements. Therefore, we consider four types of nonlinear properties of ferroelectric smart materials: nonlinear dynamics of the paraelectric–ferroelectric interphase boundaries, nonlinear equilibrium excitations—domain walls, nonlinear response of the domain structure near the first-order phase transition—wetting of domain walls—and nonlinear effects caused by external high magnetic fields. The above mentioned nonlinearities have been studied in $(Ba, Sr)TiO_3$(BST) and $Pb(Zr, Ti)O_3$(PZT). The problem is mathematically described by nonlinear parabolic equations of the reaction–diffusion type or the time-dependent Ginzburg–Landau equations. The equations are widely applied in chemical reactions and nonequilibrium phase transitions, for the description of propagation of nerve pulses, motion of domain walls, dynamics of fluctuations of the order parameter at phase transitions, self-organization phenomena and kinetics of phase transitions in liquids.

2. Concentration change in phase transition kinetics

It is well known that alloyed BST where Ba substitutes for Sr undergoes the same sequence of structural phase transitions as the pure $BaTiO_3$, but at progressively lower phase transition temperatures as the concentration of Ba is reduced [6]. At large concentrations of Ba these mixed crystals exhibit the concentration–temperature phase diagram which looks like the pressure–temperature one: the temperature ranges of stability of the tetragonal and orthorhombic phases decrease with increasing concentration of Sr and the phase transition temperature T_c moves to lower temperatures with increased dopant concentration. There is a concentration at which the character of the transition changes from first to second order. Thus, there is a range of concentrations and temperatures at which the paraelectric–ferroelectric interphase boundary exists. At a constant temperature and pressure the interface exists for

concentrations $\delta_0 < \delta < \delta^*$, where δ^* is the concentration corresponding to the stability limit of the ferroelectric phase and δ_0 is the concentration corresponding to the stability limit of the paraelectric phase; $\delta^* < \delta_t$, δ_t is the tricritical concentration of Sr. The phase transition concentration δ_c is the concentration at which the depths of the two minima of the paraelectric and ferroelectric phases are equal. We use here the Ginzburg–Landau expansion, which describes well first-order ferroelectric transitions in perovskites

$$\mathscr{F} = \int \left[f_0 + \tfrac{1}{2}\xi_1 P^2 - \tfrac{1}{4}\xi_2 P^4 + \tfrac{1}{6}\xi_3 P^6 + \Psi(\nabla P)^2 \right] d\Omega, \quad (1)$$

where $\mathscr{F}$ is the free energy, f_0 is the free energy density for the paraelectric phase, Ψ is the positive coefficient of the inhomogeneity term. For ξ_2 and $\xi_3 > 0$ Eq. (1) describes a first-order phase transition. For $\xi_2 < 0$ a second-order phase transition takes place. If $\xi_2 = 0$, a tricritical point is reached. $\xi_1 = \xi_1'(\delta)[T - T_0(\delta)]$, where T_0 is the temperature of the stability limit of the paraelectric phase. It follows from the experimental data [7] that ξ_1' increases linearly with increasing concentration of Sr. The same behavior is the case for the coefficient ξ_3 [8], while T_0 and $(T_c - T_0)$ decrease; T_c is the phase transition temperature. We can present the coefficient ξ_2 as follows:

$$\xi_2 = \xi^0(\delta_t - \delta), \quad (2)$$

where ξ^0 does not depend on δ; in the pure $BaTiO_3$ $\delta = 0$, i.e. $\xi_2 = \xi^0\delta_t$. The interphase boundary may remain quite sharp unless the concentration gets sufficiently near the tricritical point, when it becomes dispersed by fluctuations that are large in spatial extent. The temperature difference between the phase transition temperature T_c and the temperature corresponding to the stability limit of the paraelectric phase T_0 decreases with increasing concentration of Sr and this is a manifestation of the fact that the character of the phase transition changes from first to second order. The dependence Ψ vs. δ may be neglected because Ψ is proportional to the square of the lattice parameter [19] changing negligibly compared to the other composition effects at the concentration range under consideration [1]. Using the definition $\alpha = \xi_1\xi_3/\xi_2^2$, we may carry out concentrations δ_0, δ_c and δ^* from the following equations $\alpha_0 = \alpha(\delta_0) = 0$, $\alpha_c = \alpha(\delta_c) = \frac{3}{16}$, $\alpha^* = \alpha(\delta^*) = \frac{1}{4}$ which follow from the minimization of the free energy density and from the conditions for stability limits of the phases (see, for example Ref. [20]).

By changing the Sr concentration one can induce the motion of the ferroelectric interface. The above dynamics are described in terms of the time evolution of the polarization P

$$\frac{\partial P}{\partial t} = -\Gamma\frac{\delta\mathscr{F}}{\delta P}, \quad (3)$$

Γ is the kinetic coefficient which is assumed to depend noncritically on temperature, pressure and concentration. The functional derivative $\delta F/\delta P$ tends to restore the value P to its thermal value. When displaced away from the equilibrium state by changing the concentration of Sr the system will relax back to it. The kinetics of the relaxation towards equilibrium may be described in terms of the time evolution of the polarization (Eq. (3)). The solution of the kinetic equation (3) for the interface boundary conditions has the kink form [20]

$$P = \sqrt{\frac{\xi_2(1 + \sqrt{1 - 4\alpha})}{2\xi_3[1 + \exp(-\frac{S}{\Delta})]}}. \quad (4)$$

Here in Eq. (4) we use the substitution $s = x - vt$, where x is a coordinate of the boundary motion. Δ is the width of the interphase boundary given by

$$\Delta = \frac{1}{\xi_2}\sqrt{\frac{3\Psi\xi_3}{1 - 2\alpha + \sqrt{1 - 4\alpha}}} \quad (5)$$

which moves with the velocity

$$v = \frac{\Gamma\xi_2(8\alpha - 1 - \sqrt{1 - 4\alpha})}{3} \times \sqrt{\frac{2\Psi}{\xi_3(1 - 2\alpha + \sqrt{1 - 4\alpha})}}, \quad (6)$$

ξ_1 which enters α is the coefficient renormalized by the strain. The kink, described by Eq. (4), is the moving interphase boundary separating the

paraelectric ($P = 0$ at $s \to +\infty$) and ferroelectric ($P = \sqrt{\xi_2/2\xi_3(1+\sqrt{1-4\alpha})}$ at $s \to -\infty$) phases. The interphase boundary preserves its shape during the propagation because of the competition of the two terms: the homogeneous part of the free energy density tends to bring the system to a stable state, while the inhomogeneous part of Eq. (3) has the opposite tendency. The interphase boundary moves in the direction of the ferroelectric phase with decrease of Sr concentration in BST. It moves in the direction of the paraelectric phase with increasing of Sr concentration. The interphase boundary velocity v, which is shown in Fig. 1, as a function of Sr concentration and overcooling temperature, ΔT, was obtained according to Eq. (6). Parameters of these calculations could be found elsewhere (see, for example, Ref. [21]). The Sr-concentration dependence of the velocity, which is shown in Fig. 1, is calculated for $\Delta T = 25$ K. The sign of the velocity v defines the direction in which one phase grows at the expense of the other, i.e. the sign depends on the direction in which the interphase boundary propagates thus leading to formation of paraelectric or ferroelectric phases. It is seen from Fig. 1, that a change of δ up or down to the phase transition point, δ_c, induces motion of the interphase boundary. The front is in equilibrium at $\delta = \delta_c$, where the free energy densities of the two phases are equal and the velocity of the interface boundary is equal to zero.

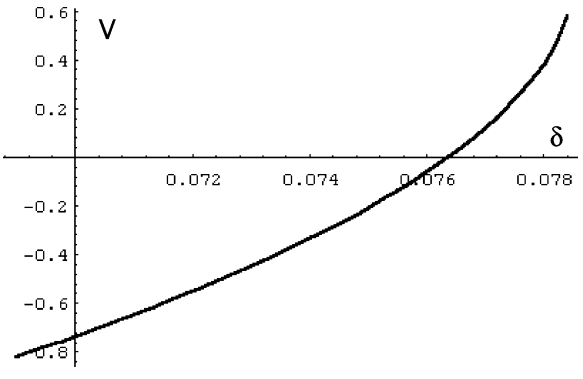

Fig. 1. The velocity of the interphase boundary v as a function of Sr concentration δ in BST. The plot corresponds to $\Delta T = 25$ K. The velocity is given in units of $\Gamma\xi_2/3[2\Psi/\xi_3]^{0.5}$.

The same behavior of interphase boundary velocity is obtained for $Pb(Zr,Ti)O_3$(PZT) for different overcooling temperatures (parameters were also taken from Ref. [21]). We show in Fig. 2 the example of calculations of values of this velocity for different concentrations of Ti dopant. These calculations were done for the overcooling temperature equal to 30 K.

The interface width and velocity are very sensitive to concentration changes. The inner plot of Fig. 2 presents the typical interphase width behavior for PZT. These effects are much stronger than the concentration influence on the phase transition temperature. Such a large sensitivity of the velocity to composition changes can provide a new method of studying the solid solutions. By varying the concentration of a component of the perovskite solid solution a ferroelectric phase growth can be controlled and the kinetics of the first-order phase transition can be governed. The present consideration can be also extended for the study of the kinetic behavior of other perovskite solid solutions including antiferroelectric ones, for example, $K(Ta,Nb)O_3$ [7] and Co-doped $BaTiO_3$ [10] because of the analogous concentration dependences of their dielectric properties. It may be also useful for the superconductive perovskite solid solutions undergoing first-order ferroelectric phase transitions. In recent years, the approach under study has been investigated experimentally and theoretically in the temperature and magnetic-field induced dynamics of ferroelectric interphase

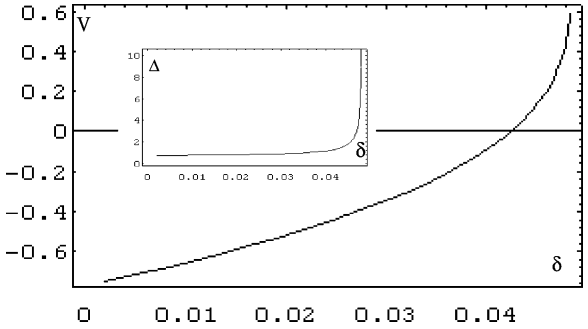

Fig. 2. The velocity of the interphase boundary v as a function of Ti concentration δ in PZT. The plot corresponds to $\Delta T = 30$ K. The velocity is given in units of $\Gamma\xi_2/3[2\Psi/\xi_3]^{0.5}$. The inner plot presents the width of the interphase boundary in units $(3\Psi\xi_3)^{0.5}/\xi_2$ vs. atomic fraction of Ti.

boundaries [17,18,22]. The measurements of the temperature dynamics are in agreement with the proposed consideration [17,18]. In addition, there are measurements on the temperature induced interface dynamics in ferroelectric $BaTiO_3$, $PbTiO_3$ and antiferroelectric $NaNbO_3$ [23–30] using polarization microscope techniques. Such diffusionless interphase boundaries are known in a number of alloys at austenitic–martensitic transformations [31]. The similarity between the two types of phase transitions [32] can be useful in describing the kinetics of martensitic transformations.

Eq. (4) describes the kink-soliton profile of the moving interphase boundary separating the paraelectric and ferroelectric phases. Thus, the above-mentioned motion of the interphase boundary is a nonlinear phenomenon. The nonlinear kinetics results from the nonlinear expression (1) for the free energy density which describes a first-order ferroelectric phase transition. Therefore, for small disturbances of external conditions the system does not necessarily relax linearly and the rate of the phase transition is described by the nonlinear kinetics equation.

3. Alloying-induced wetting of domain walls

A nonlinear alloying-induced effect on ferroelectric properties follows from the peculiarities of ferroelectric domains at first-order phase transitions. As shown in Ref. [33] the profile of the ferroelectric domain wall close to a first-order phase transition is given by

$$P = \frac{P_0 \sinh(x/\Delta')}{[f + \cosh^2(x/\Delta')]^{0.5}}. \tag{7}$$

This equation is a steady-state solution of Eq. (3) for boundary conditions

$$\lim_{x\to\pm\infty} P \to P_0,$$

$$\lim_{x\to\pm\infty} \frac{dP}{dx} \to 0. \tag{8}$$

Here the domain wall width Δ' is determined by

$$(\Delta')^2 = \frac{8\Psi\xi_3}{\xi_2^2}[1 - 4\alpha + (1 - 4\alpha)^{0.5}]^{-1} \tag{9}$$

and

$$f = 2\left[\frac{1 - 2\alpha + (1 - 4\alpha)^{0.5}}{1 - 8\alpha + (1 - 4\alpha)^{0.5}}\right]. \tag{10}$$

In Figs. 3 and 4 domain wall shapes are shown for BST with Sr concentration 7.63 at% and overcooling temperature $\Delta T = 25$ K (Fig. 3) and for PZT with Ti concentrations 4.2, 4.24 and 4.245 at% for $\Delta T = 30$ K (Fig. 4). Fig. 4 illustrates the change of the polarization kink profile with very small variation of concentrations of alloying element. We see also that for $\delta_0 \leqslant \delta \leqslant \delta_t$ a layer of the paraelectric phase appears. This phenomenon occurs with increasing temperature below T_c and is known as the wetting of the domain wall by the disordered phase [11–13]. We

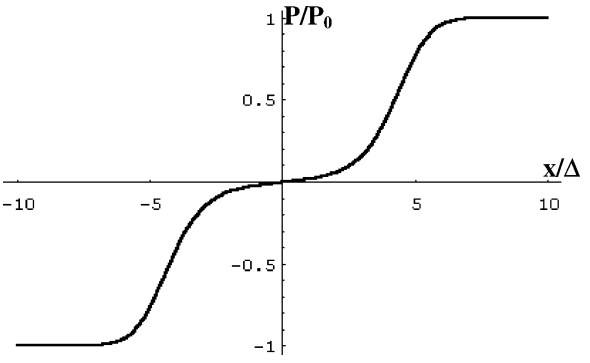

Fig. 3. The profile of the domain walls in Fig. 3. BST at Sr concentration equal to 7.63 at% and $\Delta T = 25$ K.

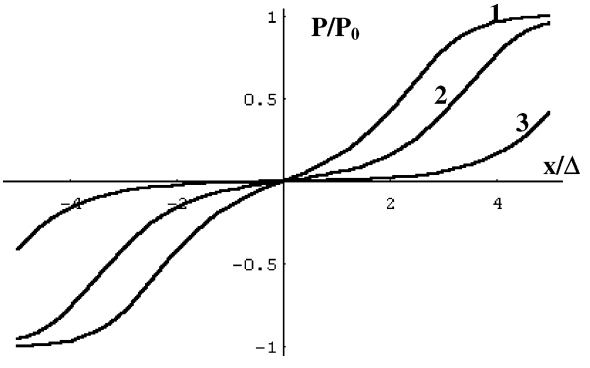

Fig. 4. The profile of the domain walls in Fig. 4. PZT at Ti concentration equal to 4.2(#1), 4.24(#2) and 4.245(#3) at% and $\Delta T = 30$ K.

see that Figs. 3 and 4 exhibit the same effect caused by alloying, i.e. the wetting of the ferroelectric domain wall by the paraelectric phase. The paraelectric phase layer in Figs. 3 and 4 is surrounded by two ferroelectric domains with opposite directions of spontaneous polarization. The fitting in Figs. 3 and 4 gives the domain wall splitting into two paraelectric–ferroelectric interphase boundaries separating between the paraelectric and ferroelectric phases and described by Eq. (4) for $t \to \infty$ in equilibrium

$$P = \frac{P_c}{[1 + \exp(x/\Delta)]^{0.5}}, \tag{11}$$

where P_c is the jump of polarization at the concentration of the phase transition δ_t. This result can be checked by direct substitution of Eq. (11) into the steady-state part of Eq. (3). The interphase boundary preserves its static shape (11) during the motion. Eq. (11) is the second particular solution of Eq. (3) for interface boundary conditions

$$\lim_{x\to+\infty} P \to 0,$$
$$\lim_{x\to-\infty} P \to P_0,$$
$$\lim_{x\to\pm\infty} \frac{dP}{dx} = 0. \tag{12}$$

We see thus that a nucleus of the paraelectric phase appears on the domain wall under the influence of the concentration change. The phenomenon can be explained as follows. The excess free energy corresponding to the domain wall (surface tension) decreases on approaching the first-order phase transition concentration δ_t. As a result, the domain wall bends to minimize the excess free energy. The growth of entropy and disorder leads to the appearance of the above layer of the paraelectric (disordered) phase. The moment of appearance of the wetting of domain walls is shown by the plot in Fig. 5. Here we see the change of the derivative of the polarization on the distance across the interphase boundary. Existence of the extremum splitting indicates the formation of the paraelectric layer in the wall.

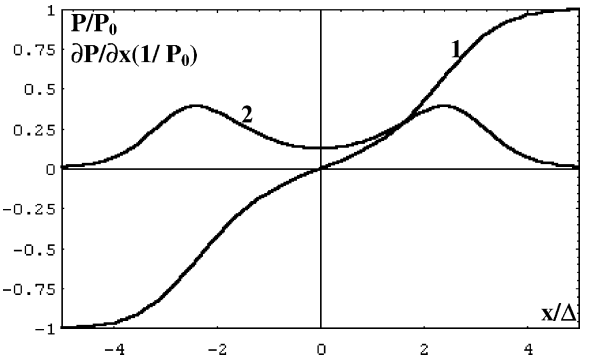

Fig. 5. The profile of the domain walls in Fig. 5. PZT (curve 1) at Ti concentration equal to 4.2 at% and $\Delta T = 30$ K and the derivative of polarization on the distance across the interphase boundary (curve 2).

4. Nonlinear magnetic field-induced effects in BST

Under the same assumption about the Landau–Khalatnikov transport coefficient Γ as in Section 2, we can study the influence of the magnetic field on the movement of the interphase boundary. This movement is determined by the equations for polarization P, the interphase boundary velocity v, and the interphase boundary width Δ (see Refs. [34–39]) and Eqs. (4)–(6) with

$$\alpha = \frac{(\xi_1 - \xi H^2 - \zeta H^4)\xi_3}{\xi_2^2}.$$

Here H is the magnetic field strength. Thus, we deal with a nonlinear magnetic field effect on the dynamics of the ferroelectric phase transitions. As is known from experiment [16] that T_0 increases with increasing magnetic field strength, coefficients ξ and ζ are associated with the magnetic field terms in the Landau–Ginzburg functional. The interphase boundary moves in the direction of the ferroelectric phase with increasing magnetic field. The interphase boundary velocity v, which is shown in Fig. 6, as a function of magnetic field, H, was carried out according to Eq. (6). The magnetic field dependence of the velocity which is shown in Fig. 6 is calculated for barium titanate BST with the atomic fraction of Sr equal to 0.01.

The sign of the velocity v defines the direction in which one phase grows at the expense of the other, i.e. the sign depends on the direction in which the

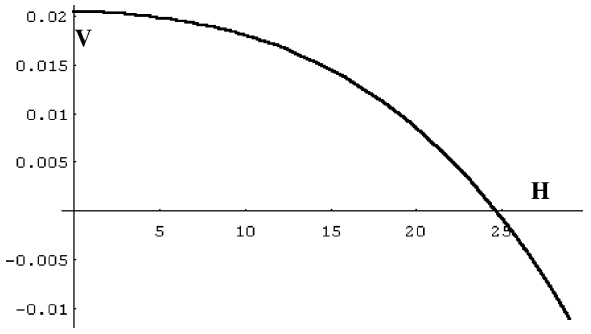

Fig. 6. The velocity of the interphase boundary v as a function of magnetic field H in Tesla. The plot corresponds to $T = 393$ K. Sr concentration is 1 at%. The velocity is given in units of $\Gamma\xi_2/3[2\Psi/\xi_3]^{0.5}$.

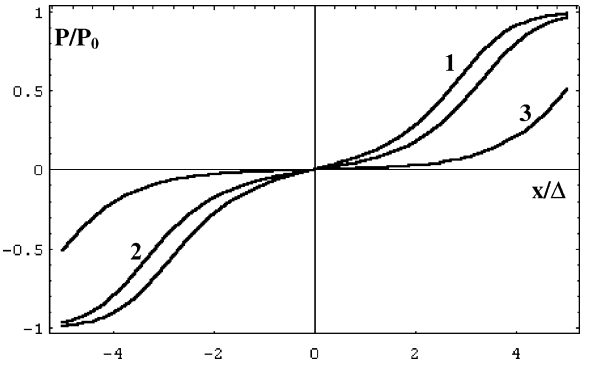

Fig. 7. The profiles of the domain walls in Fig. 7. BST at Sr concentration equal to 1.2 at%. The curves are plotted for magnetic fields 21, 20.6, and 20.35 T (curves 1, 2, and 3, respectively).

interphase boundary propagates thus leading to formation of paraelectric or ferroelectric phases. It is seen from Fig. 6, that a change of H up or down to the phase transition point induces motion of the interphase boundary. The front is in equilibrium at $H = H_c$, where the free energy densities of the two phases are equal. It would be worth to note that variation of the magnetic field from low to high values change the direction of the phase growth. The behavior of the velocity, which is plotted in Fig. 6, results from the competition of two opposite tendencies of changes of the phase transition temperature. The phase transition temperature decreases, when overcooling temperature increases, and it increases with increasing magnetic field. The ends of the velocity curve in Fig. 6 designate limits of coexistence of phases. The limits are determined from conditions $\alpha_0 = 0$ and $\alpha^* = \frac{1}{4}$. The subscript "0" refers to the temperature T_0 and magnetic field strength H_0, which determine the stability limit of the paraelectric phase. The superscript "$*$" refers to the temperature T^* and the magnetic field strength H^*, which determine the stability limit of the ferroelectric phase.

The experimental data used here for calculations are: $\xi_1'(\delta = 0)/(T - T_0) = 7.41 \times 10^{-5}$ 1/K [40], $\xi_2(\delta = 0) = 6.8 \times 10^{-13}$ cm s^2/g [40], $\xi_3 = 2.28 \times 10^{-22}$ cm^2 s^4/g^2 [40], $\xi_1/(T - T_0)(\xi_3/\xi_2^2)\xi = 6.27 \times 10^{-4}$ K/T^2[41], $\xi_1(T - T_0)(\xi_3/\xi_2^2)\zeta = 6.28 \times 10^{-7}$ K/T^4 [41]. The dependence $\Psi = \Psi(H)$ determined from a square of the lattice parameter [42] turns out to be negligible compared to the dependence of v on H, which follows from $T_0(H)$. We see that high magnetic fields accelerate the formation of the two phases. Despite small shift of the phase transition temperature under the influence of magnetic fields (the shift is about 0.3 K at $H =$ 20 T in $BaTiO_3$ [41] the magnetic field effect on the interphase boundary velocity is very large. Therefore, the use of high magnetic fields results in larger shifts of ferroelectric phase transitions and in considerable increase of the rate of phase growth. This large magnetic field effect takes place close to the phase transition point even for relatively small fields within the range of coexistence of metastable and stable phases. It occurs because each slight change of the external magnetic field leads to substantial change of the free energy density in the region of coexistence of ferroelectric and paraelectric phases. We calculated domain profiles in BST with Sr-concentration equal 1.2 at% according to Eq. (7). These profiles in fields 20.35, 20.6 and 21.0 T are shown in Fig. 7. It is seen from our results that with approaching a critical magnetic field at $T = 392$ K the wetting takes place in BST. It is easy to see how the magnetic field influences the thickness of the layer of a paraelectric BST phase which wets the domain wall between two ferroelectric domains with opposite polarization. The width of the paraelectric layer decreases when the external

magnetic field increases. The effect is strong. This result is very important, showing that the external magnetic field may be used as a tool changing the fine domain structure of the alloyed perovskites. This influence can be detected by measuring the optical, dielectric, mechanical and other properties of the alloyed perovskites in the vicinity of the phase transition temperature.

5. Conclusion

We presented a study of the alloying- and magnetic field-induced kinetics of ferroelectric phase transitions. Our research is based on the exact solution of the time-dependent Ginzburg–Landau equation. In Figs. 1, 2 and 6 we showed the effect of slowing down of the interphase boundary motion at the phase transition point. We demonstrated that the influence of magnetic fields on the interphase boundary dynamics in the metastable region is large although the magnetic field shift of the ferroelectric phase transition point is relatively small. We studied the wetting phenomena of ferroelectric domain walls induced by alloying and magnetic field tuning. An equilibrium size of the paraelectric phase nucleus in the domain wall is a result of the competition of long- and short-range forces. Their balance is sensitive to changes of a dopant concentration or external magnetic field. We considered a strongly nonlinear effect: the large response of the paraelectric layer width to a comparatively small change of the external magnetic field. This drastic change in the width of the paraelectric layer is caused by the critical dependence of the paraelectric layer width. The usual logarithmic divergence of the wetting layer with respect to the excess free energy holds. The alloying-induced wetting of the ferroelectric domain wall at the first-order paraelectric phase transition is shown to take place indicating the splitting of a domain wall into two interphase boundaries separating the paraelectric phase and the polarization-up and polarization-down regions. Two-domain regions of polarization of opposite signs may be developed in ferroelectrics with long-range order. A paraelectric phase can appear at domain interfaces. Thus, the paraelectric phase can wet domain walls in the ferroelectric phase near a first-order phase transition point. The wetting can be produced by altering composition, temperature, pressure, or external magnetic filed. Therefore, we studied new features of domain walls expected due to the degeneracy of the electrically ordered structure.

Our research demonstrated that magnetic field serves as a tool refining the ferroelectric domain structure. The presence of a wetting layer leads to a new length scale, which is given by the wetting layer thickness, i.e. by the separation of two interfaces bonding this layer. It typically varies from the critical value, which may be very small up to hundreds of nanometers sufficiently close to the interface. From our point this data on highly interesting nonlinear properties of smart perovskites may be a way of producing a very fine domain structure in these technologically important materials.

$(Ba, Sr)TiO_3$ and $Pb(Zr, Ti)O_3$ are tetragonal ferroelectrics and have six polarization directions. The domain walls in these materials are not only 180° but also 90° walls. The last case would be studied in the nearest future and demands a thorough treatment of the experimental parameters for the Ginzburg–Landau functional. The change of these parameters and relations between them may influence the wetting effect. For 90° walls, the elastic strain energy is very important.

One additional note has to be done concerning the influence of elastic fields on the phenomenon of wall wetting. In our study the strain-dependent terms formally were not included in the free energy density and we did not investigate them directly in the framework of the applied formalism. In the paper of Lajzerowicz [13] it was shown that account for strains suppress the effect of splitting of a domain wall. There are several circumstances that make our results valuable: (a) a magnetic field does not influence on the strain distribution because of the absence of magnetostriction effects in BST and PZT; (b) strain effects accompany phase transitions in perovskite ferroelectrics, the parameters of Landau–Ginzburg functional were taken from experiments. Thus they include effectively the influence of elastic fields on formation of paraelectric nuclei.

The same happens in the study of alloying effect on the wetting of domain walls. The elastic accommodation is effectively included in parameters of the functional and partially is accounted by experimentally estimated derivatives $(dT_0/d\delta)$. For small concentrations of alloying elements the terms accounting for alloying are small in comparison with those of the same power in polarization and do not delete the effect of wetting. The detailed study of importance of elastic fields in magnetic field- or composition-induced wetting of domain walls could be done if the experimental data on the parameters of the free energy density functional would be available. To the best of our knowledge until present time, these data have been absent and only qualitative estimations may be done.

The restructuring of domain walls preceding the formation of the paraelectric phase can be studied by methods based on the change in the character of resonance in domains and domain walls. The formation of nuclei of the paraelectric phase should be signalized by the appearance of an additional resonance line of the spectrum.

References

[1] M.E. Lines, A.M. Glass, Principles and Application of Ferroelectrics and Related Materials, Clarendon Press, Oxford, 1977.
[2] A.W. Sleight, J.L. Gillson, P.E. Bierstedt, Solid State Commun. 17 (1975) 27.
[3] J. Robertson, G. A. Samara, P.S. Peercy, Solid State Phys. 36 (1981) 1.
[4] W.L. Warren, B.A. Tuttle, D. Dimos, D. Smyth, Appl. Phys. Lett. 63 (1993) 1519.
[5] P.F. Baude, C. Ye, D.L. Polla, Appl. Phys. Lett. 64 (1994) 2670.
[6] R.W. Whatmore, C. Clarke, A.M. Glazer, J. Phys. C 11 (1978) 3089.
[7] S. Triebwasser, Phys. Rev. 114 (1959) 63.
[8] K. Bethe, F. Welz, Mater. Res. Bull. 6 (1971) 209.
[9] R. Clarke, Phys. Rev. B 18 (1978) 4920.
[10] L. Benguigui, Y. Beaucamps, Phys. Rev. B 23 (1981) 5866.
[11] J.W. Cahn, J. Chem. Phys. 66 (1977) 3667.
[12] B. Widom, J. Chem. Phys. 68 (1978) 3878.
[13] J. Lajzerowicz, Ferroelectrics 35 (1981) 219.
[14] G.T. Rado, V.J. Folen, Phys. Rev. Lett. 7 (1961) 310.
[15] E. Ascher, H. Rieder, H. Schmid, H. Stössel, J. Appl. Phys. 37 (1966) 1404.
[16] W.N. Lawless, C.F. Clark, S.L. Swartz, Ferroelectric Lett. 44 (1982) 121.
[17] J. Dec, Ferroelectrics 89 (1989) 193.
[18] J. Dec, V.E. Yurkevich, Ferroelectrics 110 (1990) 77.
[19] V.L. Ginzburg, Sov. Phys. Sol. Stat. 2 (1960) 1123.
[20] A. Gordon, Phys. Lett. 99 (1983) 329.
[21] A. Gordon, S. Dorfman, D. Fuks, Phil. Mag. A 75 (1997) 1391.
[22] A. Gordon, P. Wyder, Phys. Rev. B 46 (1992) 5777.
[23] J.C. Burfoot, T.J. Parker, Br. J. Appl. Phys. 17 (1966) 213.
[24] V.M. Fridkin, M.I. Gorelov, A.A. Grekov, V.A. Lyakhovitskaya, A.I. Rodin, Sov. Phys. JETP Lett. 4 (1966) 310.
[25] S.M. Yufatova, Y.G. Sindeyev, V.G. Gavrilyatchenko, E.G. Fesenko, Ferroelectrics 26 (1980) 809.
[26] Z. Surowiak, J. Dec, V.G. Gavrilyatchenko, A.F. Semenchev, E.G. Fesenko, Sov. Phys. Sol. Stat. 20 (1978) 1409.
[27] Z. Surowiak, R. Skulski, V.G. Gavrilyatchenko, A.F. Semenchev, E.G. Fesenko, Sov. Phys. Sol. Stat. 20 (1978) 1411.
[28] J. Dec, Ferroelectrics 69 (1986) 187.
[29] J. Dec, J. Phys. C 21 (1988) 1257.
[30] J. Dec, J. Kapulinski, Phase Transitions 18 (1989) 1.
[31] J.W. Christian, The Theory of Transformations in Metals and Alloys, Pergamon, Oxford, 1975.
[32] F. Falk, J. de Phys. C-4 43 (1982) 3.
[33] I.I. Ivanchik, Sov. Phys. Solid State 3 (1962) 2705.
[34] A. Gordon, S. Dorfman, Phys. Rev. B 50 (1995) 13 132.
[35] A. Gordon, S. Dorfman, Phys. Rev. B 51 (1995) 15 661.
[36] A. Gordon, S. Dorfman, Phys. Rev. B 51 (1995) 9306.
[37] A. Gordon, S. Dorfman, P. Wyder, Phys. Rev. B 52 (1995) 143.
[38] S. Dorfman, D. Fuks, A. Gordon, A.V. Postnikov, G. Borstel, Phys. Rev. B 52 (1995) 7135.
[39] S. Dorfman, D. Fuks, A. Gordon, Phys. Rev. B 52 (1995) 12 473.
[40] W.J. Merz, Phys. Rev. 91 (1953) 513.
[41] D. Wagner, D. Bauerle, Phys. Lett. A 83 (1981) 347.
[42] R. Clarke, L. Benguigui, J. Phys. C 10 (1977) 1963.